

633 nm 内腔式 He-Ne 激光器热-频率特性研究

席路¹, 殷聪^{1*}, 王建波¹, 石春英¹, 蔡山¹, 刘若男^{1,2}, 李孟瑶^{1,3}, 张超超^{1,2}¹中国计量科学研究院几何量计量科学研究所, 北京 100029;²中国计量大学计量测试工程学院, 浙江 杭州 310018;³北京理工大学光电学院, 北京 100081

摘要 研究了在-20~40 °C 环境温度下 633 nm 内腔式 He-Ne 激光管的自由运转特性, 设计了激光器系统的预热和稳频控制方案, 实现了 633 nm 内腔式 He-Ne 激光器的频率稳定。当室温约为 24 °C 时, 锁定后的热稳频激光器与高精度碘稳定激光器的拍频结果显示, 3 h 内频率的相对标准不确定度为 $u = 6.4 \times 10^{-9}$, 阿伦方差为 7.0×10^{-11} (采样时间 $\tau = 1$ s), 3 个月内的频率复现性优于 4.6×10^{-9} 。研究了在-20~40 °C 范围内不同环境温度下锁定后输出激光的频率漂移规律, 实验结果显示, 稳频后激光输出频率随环境温度的漂移量约为 293 kHz/°C, 与采用压力估算模型计算得到的漂移值 268 kHz/°C 相一致。因此, 当激光器工作在一个较大的温度范围内时, 可以通过插值校准来获得更准确的参考输出频率。

关键词 激光器; 内腔式 He-Ne 激光器; 双纵模; 功率平衡; 高低温试验; 频率漂移

中图分类号 TN242; TN248.2; TN249

文献标志码 A

doi: 10.3788/CJL202249.0601002

1 引言

稳频 He-Ne 激光器作为许多激光干涉仪的光源, 目前已被广泛应用于计量与测量领域^[1-2]。内腔式 633 nm He-Ne 激光管由于具有结构简单、工作性质稳定、使用寿命长、价格较低等特点, 常被用于稳频 He-Ne 激光器的研究中^[3-11]。1972 年, Balhorn 等^[12] 根据内腔式 He-Ne 激光管输出纵模增益与频率的关系, 首次提出了双纵模功率平衡稳频原理, 并在 633 nm 内腔式 He-Ne 激光管中实现了激光频率的稳定, 相对频率变化量小于 1×10^{-7} 。

双纵模功率平衡稳频原理利用激光介质增益曲线中频率与功率的关系, 将两个纵模稳定在增益曲线中心频率两侧的等功率点处。这一原理的本质是以增益曲线的中心频率为基准进行稳频控制, 但是管内气压会影响增益曲线的中心频率, 因此, 稳频后的激光频率与管内气压有关。Niebauer^[13] 提到, 腔内压力变化对多普勒线宽的影响约为 112.5 kHz/Pa, 对中心频率的影响约为 135.0 kHz/Pa。对于全内

腔式 He-Ne 激光管而言, 腔内气压的变化主要是温度改变引起的, 腔内气压随温度的增加而线性增加, 因此激光管输出激光的频率与温度密切相关。研究者在长度分别为 21.6 cm 和 14.9 cm 的两个内腔式 He-Ne 激光管上测试了温度对频率的影响, 当长管加热升温为 1 °C 左右时, 频率漂移 280 kHz, 频率随温度的漂移量为 280 kHz/°C; 短管加热升温 5 °C 时, 频率漂移 1.74 MHz, 频率漂移量为 348 kHz/°C。频率随温度的漂移现象也出现在内腔式塞曼型稳频激光器中, Zumberge 等^[14-15] 对塞曼稳频激光器长期研究后发现, 温度对频率的影响大小为 0.2~0.6 MHz/°C, 相对频率漂移约为 $10^{-9}/\text{°C}$ 。

这些研究结果都揭示了激光频率随温度漂移的规律, 但是大多实验都是在室温下进行的, 稳频 He-Ne 激光器的使用范围越来越广泛, 对稳频激光器的环境适应性又有了更高的要求。例如, 激光干涉绝对重力仪中所使用的稳频 He-Ne 激光器需要在不同的环境温度下工作^[16-17]。因此, 目前的稳频 He-Ne 激光器在极端温度下的频率准确度受到了

收稿日期: 2021-07-28; 修回日期: 2021-08-24; 录用日期: 2021-08-30

基金项目: 国家重点研发计划(2021YFF0603300、2016YFF0200302)、国家自然科学基金(62075165)

通信作者: *yincong@nim.ac.cn

很大的限制。

本文基于全内腔式 He-Ne 激光管的特性,采用双纵模功率平衡稳频原理,设计了基于加热膜调谐激光频率的 633 nm He-Ne 激光器热稳频控制系统,并在 $-20\sim 40\text{ }^{\circ}\text{C}$ 的环境温度下,实现了 633 nm 内腔式 He-Ne 激光管的稳频控制,同时还研究了稳频后激光器的热-频率特性,以提高不同环境温度下激光参考输出频率的准确度。

2 激光稳频原理与结构设计

2.1 双纵模功率平衡稳频原理

激光器输出激光的谐振频率满足

$$\nu_q = q \frac{c}{2nl}, \quad (1)$$

式中: q 是正整数; c 是真空中光速(m/s); n 是激光介质的折射率; l 是谐振腔长度(m)。由于激光在谐振腔内会产生衍射、散射等多种损耗,因此只有增益大于阈值条件的纵模才能输出,如图 1 所示。

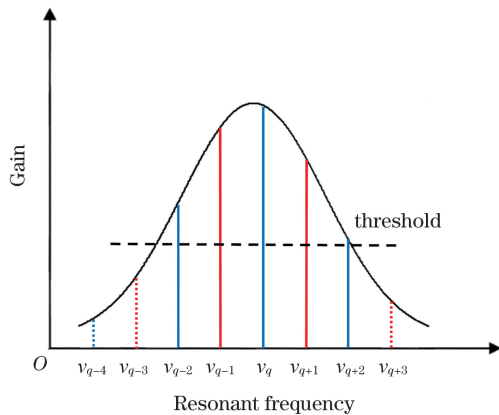


图 1 He-Ne 激光管的纵模分布

Fig. 1 Longitudinal mode distribution of He-Ne laser tube

由(1)式可得,相邻两个纵模的频率间隔为

$$\Delta\nu_q = \frac{c}{2nl}. \quad (2)$$

由(2)式可知,纵模间隔 $\Delta\nu_q$ 与腔长 l 成反比。因此可以通过缩短腔长 l 来增大 $\Delta\nu_q$,使得在增益曲线阈值以上的纵模只有 2 个。由(1)式可知,激光器频率稳定度由腔长 l 的稳定度和腔内介质折射率 n 的稳定度共同决定。在激光器处于近似热平衡状态时,腔内介质的折射率变化不大,因此可以通过微调腔长来获得较高的频率稳定度。当激光管工作时,控制谐振腔的长度,使两个纵模在增益曲线上的增益相等,这样两个纵模就被稳定在固定的位置上,输出频率保持稳定,这就是双纵模功率平衡稳频原理,如图 2 所示,其中 ν_0 为增益曲线的中心频率,

$[\nu'_q, \nu''_q]$ 为 ν_q 的波动范围, $[\nu'_{q+1}, \nu''_{q+1}]$ 为 ν_{q+1} 的波动范围。

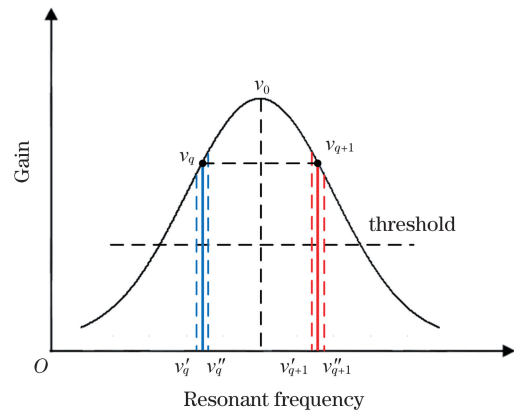


图 2 He-Ne 激光管的增益-频率曲线(双纵模)

Fig. 2 Gain-frequency curve of He-Ne laser tube

(double longitudinal mode)

2.2 激光稳频系统的结构设计

系统选用的激光管是 633 nm 全内腔式商用 He-Ne 激光管,腔长约为 137 mm,谐振腔内可同时存在两个纵模,纵模频率间隔约为 1090 MHz,两个纵模的偏振方向相互垂直。为了不影响阳极的输出光,我们使用了阴极的尾光作为反馈检测光,尾光功率足以满足检测和控制的要求。尾光经过偏振分光器后被分为两束偏振方向相互垂直的偏振光,随着腔的调谐,当一个偏振态的光功率增加时,与其正交的另一偏振态的光功率相应降低。两束偏振光被一个二象限光电接收器接收,以两束偏振光的等功率点为参考点,控制谐振腔的腔长,使两个纵模保持在功率相等的状态,以获得稳定的激光输出频率。

采用加热膜控制腔长的双纵模热稳频法的稳频结构示意图如图 3 所示。633 nm 全内腔式 He-Ne 激光管输出的尾光被沃拉斯顿棱镜分为两束偏振方向相互垂直的线偏振光,之后两束线偏振光分别入射到一个二象限光电接收器上,光电接收器检测两束线偏振光的功率并将其转化为电信号输出。光电接收器输出的信号经过信号调理电路后被模数(A/D)转换器采集并输入到微控制器(MCU)中,微控制器根据两束线偏振光的功率差输出控制量给数模(D/A)转换器,数模转换器控制加热膜驱动电路,通过加热膜控制谐振腔腔长,从而实现输出激光的频率稳定。激光管管壁和激光器外部均有一个温度检测器件,用来检测激光管的温度和环境温度。激光管阳极输出的双纵模激光通过一个偏振片后只保留一个线偏振光,此线偏振光即为频率稳定的单纵模输出光。

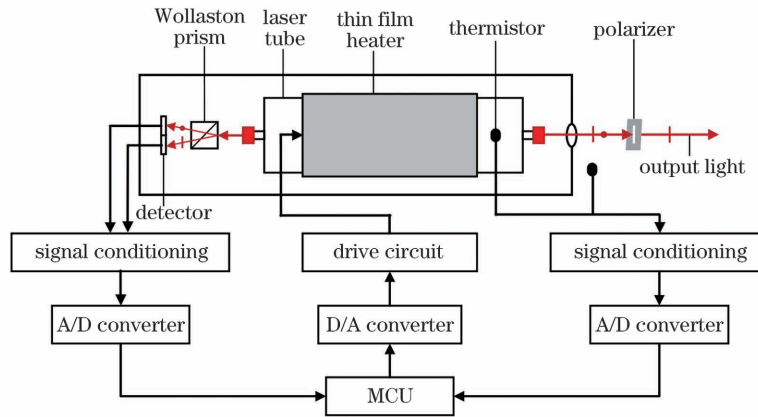


图 3 双纵模热稳频法的稳频结构示意图

Fig. 3 Structural diagram of frequency stabilization for double longitudinal mode thermal frequency stabilization method

3 激光管自由运转的热特性

为了进行稳频控制,我们研究了激光管自由运转时,两个纵模的电压差值和激光管温度随时间的变化规律。实验时环境温度约为 24 °C,激光管管壁的初始温度为 24.08 °C,点亮激光管,使其处于自由运转的状态,激光管的工作电流约为 3.7 mA,通过光电接收器检测两个纵模的功率变化。在自由运转过程中,激光管因放电电流的加热作用,管壁温度会逐渐上升,因此激光管谐振腔沿光轴方向伸长,输出的两个纵模频率向低频方向漂移,当一个纵模在增益曲线的低频侧消失时,另一个纵模在增益曲线的高频侧出现,两个纵模的电压差值每通过零点一次,腔长增加 $\lambda/2$ (λ 表示激光波长),电压差值的大小随谐振腔的变化呈现出周期性改变。随着激光管预热时间的加长,系统的热交换趋于平衡,根据纵模电压差两次经过零点的时间间隔可以看出,腔长膨胀

速率在变缓,两个纵模的频率漂移也在变缓,同时管壁温度也在逐渐趋于平衡,不再上升,系统达到近似热平衡状态。激光管在自由运转状态下,输出的两个纵模的电压差值和激光管温度随时间的变化规律如图 4 所示。实验结果显示,激光管从室温状态下的自由运转到近似热平衡状态时,双纵模的电压差值变化了 40 个周期,腔长的增量 $\Delta l = 633 \text{ nm} \times 40$,初始状态时,电压差值变化 1 个周期用时 0.35 min,腔长的膨胀速率可以计算为

$$v = \frac{\lambda}{0.35 \text{ min}} = 1808.57 \text{ nm} \cdot \text{min}^{-1}. \quad (3)$$

达到近似热平衡状态时,电压差值变化 1 个周期用时 25.37 min,腔长的膨胀速率变为

$$v' = \frac{\lambda}{25.37 \text{ min}} = 24.95 \text{ nm} \cdot \text{min}^{-1}. \quad (4)$$

经过约 1 h 后,激光管的温度基本达到平衡,热平衡时管壁的温度为 53.19 °C。

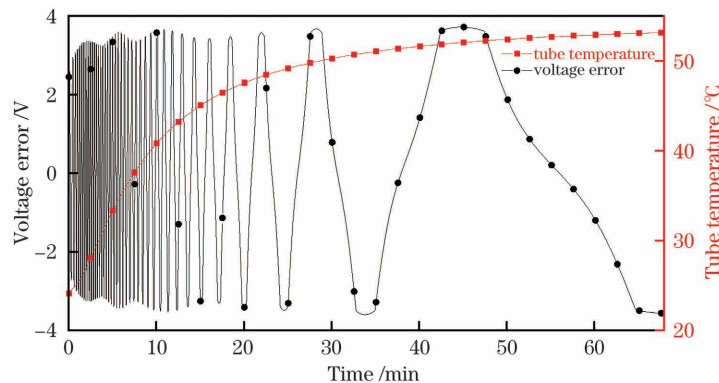


图 4 双纵模电压差值和激光管温度随时间的变化

Fig. 4 Voltage error between two longitudinal modes and laser tube temperature versus time

我们还在 -20 ~ 40 °C 温度范围内研究了不同环境温度下激光管的自由运转过程。将激光器放置在高低温试验箱中,设置不同的环境温度,等待激光

器温度与环境温度相等后,点亮激光器使其充分预热,测得系统达到热平衡后激光管的管壁温度与初始环境温度的关系,如图 5 所示。可以看出,二者呈

线性关系,这表明即使激光器处于不同的环境温度下,由于激光器系统与外界环境的热交换能力近似不变,因此最终达到热平衡时激光管管壁的温度与初始环境温度是一个固定的差值。此外,在不同的环境温度下,激光管达到近似热平衡状态时,双纵模的电压差值都变化了 40 个周期,腔长的热膨胀速率也相同,这同样说明了热平衡状态时,激光器系统的发热与散热比是恒定的,这一特性对我们在大范围环境温度变化下进行稳频控制、设计稳频控制方案是有帮助的。

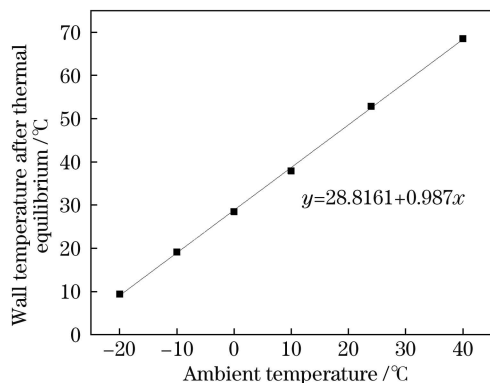


图 5 激光管达到热平衡后的管壁温度与环境温度的关系

Fig. 5 Relationship between wall temperature after thermal equilibrium for laser tube and ambient temperature

4 稳频锁定的热-频率特性

根据对 633 nm 内腔式 He-Ne 激光管的热特性分析,设计了激光器系统的稳频控制方案。稳频控制过程分为两个阶段,第一阶段是预热阶段,第二阶段是稳频控制阶段。预热阶段通过加热膜将激光管加热到设定状态,由于激光管在不同环境温度下达到近似热平衡状态时,双纵模的电压差值都变化了 40 个周期,因此可以以一个固定的周期数作为预热阶段的设定值,当双纵模的电压差值变化的周期数达到设定值时,可进行稳频控制。预热阶段完成后,切换为稳频控制阶段,稳频控制阶段以两个纵模转换的电压差为反馈量,以电压差零点为设定值,通过加热膜控制腔长,形成闭环控制,使两个纵模功率相等,最终输出稳定的激光频率。

在室温下,激光管管壁的初始温度约为 24 °C,经过预热后将其锁定,预热和锁定过程中两个纵模的电压差信号随时间的变化如图 6 所示。实验结果表明,激光器的预热时间约为 3 min,3 min 后,激光器实现锁定。

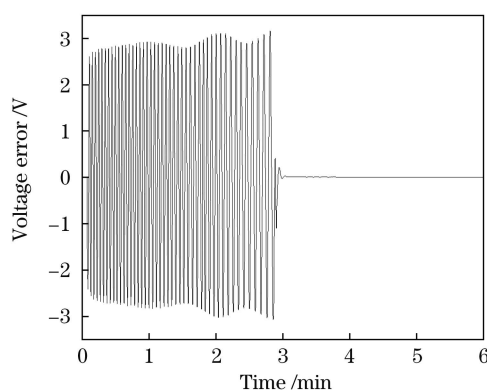


图 6 激光器的预热和锁定过程

Fig. 6 Laser preheating and locking process

对输出激光的频率进行拍频实验,参考激光波长为中国计量科学研究院 633 nm 碘稳频 He-Ne 激光波长基准,相对标准不确定度 $u = 2 \times 10^{-11}$,测得的频率波动和阿伦方差分别如图 7 和图 8 所示。实验结果显示,在 3 h 内,锁定后激光器平均频率的波动范围为 ± 1.5 MHz,采样时间 $\tau = 1$ s 时对应的阿伦方差为 7.0×10^{-11} ,在采样时间 $0.1 \text{ s} \leq \tau \leq 2000 \text{ s}$ 内,阿伦方差优于 4.3×10^{-10} 。

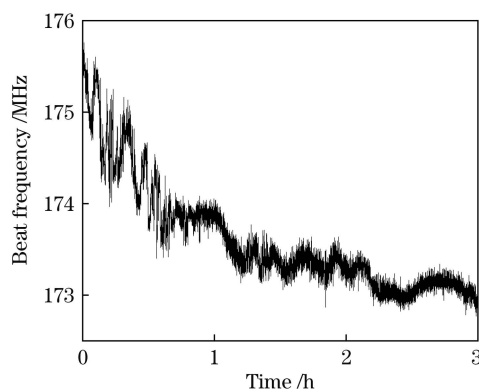


图 7 稳定状态下激光频率的拍频曲线

Fig. 7 Beat frequency curve of laser frequency in steady state

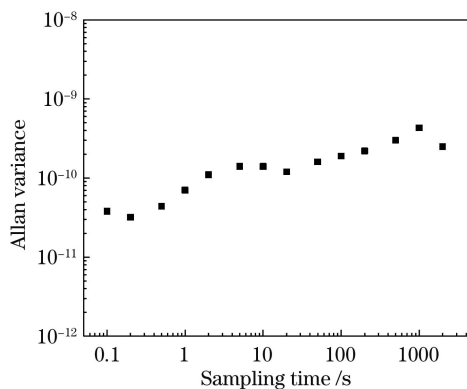


图 8 稳定状态下激光频率的阿伦方差

Fig. 8 Allan variance of laser frequency in steady state

我们还在 3 个月的时间里开展了 6 组频率复现性实验,环境温度为 $T=(24\pm 2)^{\circ}\text{C}$,每次测量时间大于 1 h,考察 633 nm 内腔式 He-Ne 激光器热稳频控制系统的频率复现性,测得的拍频结果如图 9 所示,6 次拍频实验结果的平均值为 173.607 MHz,其中最大值和最小值分别为 174.869 MHz 和 172.705 MHz,两者之差为 2.164 MHz,频率复现性优于 4.6×10^{-9} 。在环境温度变化不大的情况下,激光器具有良好的复现性。

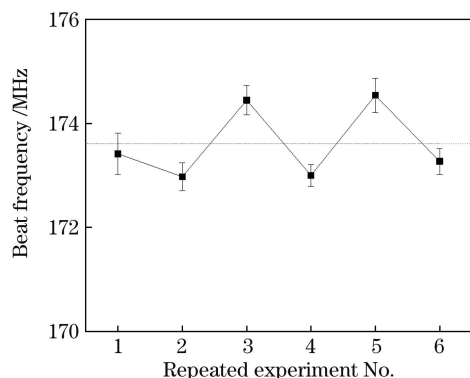


图 9 稳定状态下激光频率重复性实验结果

Fig. 9 Experimental result of laser frequency repeatability in steady state

此外,还研究了环境温度对稳频结果的影响。我们设置了不同的环境温度进行稳频实验,环境温度为 $-20\sim 40^{\circ}\text{C}$,间隔约为 20°C ,测量在不同环境温度下稳频后激光管管壁的温度和拍频值,实验结果分别如图 10 和图 11 所示。实验结果显示,稳频后激光管管壁的温度随环境温度发生变化,二者呈线性关系;同时,稳频后激光器输出的频率随环境温度的漂移量约为 $+293\text{ kHz}/^{\circ}\text{C}$ 。经过线性插值校准后,当环境温度为 23.7°C 时,实际频率值与经过插值校准后的参考输出频率值相差 1.81 MHz,在其余温度点,实际频率值与参考输出频率值的差值均小于 1.81 MHz。

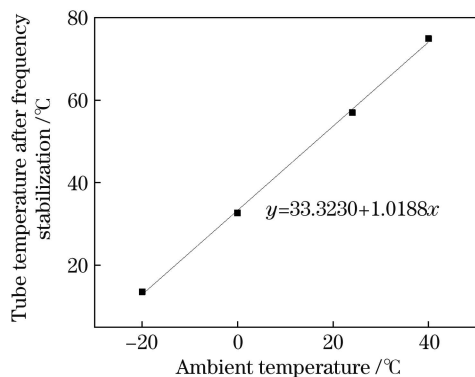


图 10 稳频后激光管管壁的温度随环境温度的变化

Fig. 10 Laser tube temperature versus ambient temperature after frequency stabilization

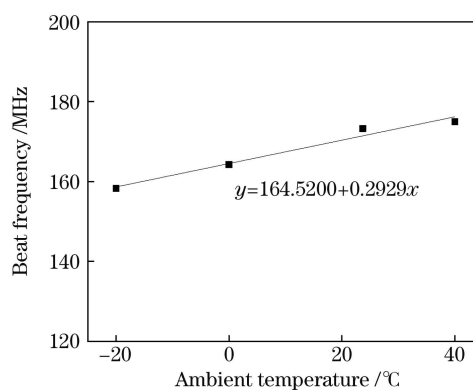


图 11 激光频率随环境温度的漂移

Fig. 11 Shift of laser frequency with ambient temperature

由于激光管是内腔式结构,管内温度与压强呈线性关系,腔内压力变化会对多普勒宽度和增益曲线中心频率产生影响,对多普勒线宽的影响约为 $112.5\text{ kHz}/\text{Pa}$,对增益曲线中心频率的影响约为 $135.0\text{ kHz}/\text{Pa}$ 。研究者在 633 nm He-Ne 激光管中测量了不同气体混合物的压力诱发的频率偏移,发现氦的正压偏移为 $(165.0\pm 22.5)\text{ kHz}/\text{Pa}$,而氖的正压偏移为 $(-187.5\pm 37.5)\text{ kHz}/\text{Pa}$,实际的频率漂移与激光管内这两种气体的分压比有关^[13]。对于体积比为 9:1 的氦氖气体混合物,利用氦氖气体的正压偏移值,通过计算可以得到实际的频率漂移值为 $129.8\text{ kHz}/\text{Pa}$,同时可估算出 1°C 温度变化引起的频移。假设管的标称温度和压强分别为 323 K 和 666.6 Pa,根据温度和气压的变化关系,可计算得到由温度引起的频率漂移量约为 $268\text{ kHz}/^{\circ}\text{C}$,这个简单的压力漂移模型与我们观察到的平均锁定频率的温度依赖性一致。因此,如果激光器工作在一个较大的温度范围内(如 $-20\sim 40^{\circ}\text{C}$),频率变化量可能达到 16 MHz,频率复现性仅为 3.4×10^{-8} 。对于一些复现性要求较高的稳频激光器系统,频率漂移是难以接受的,就需要通过插值或其他频率补偿方法来修正频率随温度的漂移,以获得更准确的参考输出频率。

5 结 论

研究了在 $-20\sim 40^{\circ}\text{C}$ 环境温度下 633 nm 内腔式 He-Ne 激光管的自由运转特性。实验结果表明,在不同环境温度下,激光管达到热平衡状态时,激光管温度与环境温度的差值固定,膨胀速率也相同,且双纵模电压差变化了相同的周期。根据这些特性,设计了激光器系统的预热和稳频控制方案,实现了

633 nm 内腔式 He-Ne 激光器的频率稳定。当室温约为 24 °C 时,锁定后的热稳频激光器与高精度碘稳定激光器的拍频结果显示,3 h 内频率的相对标准不确定度为 $u=6.4\times 10^{-9}$, $\tau=1$ s 时对应的阿伦方差为 7.0×10^{-11} ,当采样时间为 $0.1\text{ s}\leq\tau\leq 2000$ s 时,阿伦方差优于 4.3×10^{-10} ,3 个月内的频率复现性优于 4.6×10^{-9} 。还研究了在 $-20\sim 40$ °C 环境温度下锁定后输出激光的频率漂移规律。实验结果显示,稳频后激光管管壁的温度随环境温度发生变化,二者呈线性关系;同时,稳频后激光器输出的频率随环境温度的漂移量约为 293 kHz/°C,与采用压力估算模型计算得到的漂移值 268 kHz/°C 一致。因此,当激光器工作在一个较大的温度范围内(如 $-20\sim 40$ °C)时,可以通过插值校准以获得更准确的参考输出频率。

参 考 文 献

- [1] Zhang P, Cui J J. Research progress in nonlinear error compensation suppression and measurement of heterodyne interferometer [J]. Laser & Optoelectronics Progress, 2021, 58(11): 1100003.
张鹏, 崔建军. 外差干涉仪非线性误差补偿抑制与测量研究进展[J]. 激光与光电子学进展, 2021, 58(11): 1100003.
- [2] Yu H J, Zhao G G. Improving measurement accuracy of dual-frequency laser interferometer based on vibration node optimization [J]. Laser & Optoelectronics Progress, 2020, 57(15): 151202.
于海娇, 赵国罡. 基于振动节点优化提高双频激光干涉仪的测量精度[J]. 激光与光电子学进展, 2020, 57(15): 151202.
- [3] Diao X F, Tan J B, Hu P C, et al. Frequency stabilization of an internal mirror He-Ne laser with a high frequency reproducibility [J]. Applied Optics, 2013, 52(3): 456-460.
- [4] Qian J, Liu Z Y, Shi C Y, et al. Frequency stabilization of internal-mirror He-Ne lasers by air cooling [J]. Applied Optics, 2012, 51(25): 6084-6088.
- [5] Seta K T, Iwasaki S. Frequency stabilization of a He-Ne laser using a thin film heater coated on the laser tube [J]. Optics Communications, 1985, 55(5): 367-369.
- [6] Ogasawara H, Nishimura J. Frequency stabilization of internal-mirror He-Ne lasers [J]. Applied Optics, 1983, 22(5): 655-657.
- [7] Sasaki A, Hayashi T. Amplitude and frequency stabilization of an internal-mirror He-Ne laser [J]. Japanese Journal of Applied Physics, 1982, 21(10): 1455-1460.
- [8] Ogasawara H, Nishimura J. Frequency stabilization of internal-mirror He-Ne lasers by a flowing-water method [J]. Applied Optics, 1982, 21(7): 1156-1157.
- [9] Yoshino T. Frequency stabilization of internal-mirror He-Ne ($\lambda = 633$ nm) lasers using the polarization properties [J]. Japanese Journal of Applied Physics, 1980, 19(11): 2181-2185.
- [10] Umeda N, Hirano I, Togawa M, et al. Polarization mode and frequency stabilization of an internal mirror laser [J]. Oyobuturi, 1978, 47(1): 42-49.
- [11] Bennett S J, Ward R E, Wilson D C. Comments on: frequency stabilization of internal mirror He-Ne lasers [J]. Applied Optics, 1973, 12(7): 1406.
- [12] Balhorn R, Kunzmann H, Lebowsky F. Frequency stabilization of internal-mirror helium-neon lasers [J]. Applied Optics, 1972, 11(4): 742-744.
- [13] Niebauer T M, Faller J E, Godwin H M, et al. Frequency stability measurements on polarization-stabilized He-Ne lasers [J]. Applied Optics, 1988, 27(7): 1285-1289.
- [14] Zumberge M A. Frequency stability of a Zeeman-stabilized laser [J]. Applied Optics, 1985, 24(13): 1902-1904.
- [15] Sasagawa G S, Zumberge M A. Five-year frequency stability of a Zeeman stabilized laser [J]. Applied Optics, 1989, 28(5): 824-825.
- [16] Niebauer T M, Hoskins J K, Faller J E. Absolute gravity: a reconnaissance tool for studying vertical crustal motions [J]. Journal of Geophysical Research Atmospheres, 1986, 91(B9): 9145-9149.
- [17] Wu S Q, Li T C. Technical development of absolute gravimeter: laser interferometry and atom interferometry [J]. Acta Optica Sinica, 2021, 41(1): 0102002.
吴书清, 李天初. 绝对重力仪的技术发展: 光学干涉和原子干涉 [J]. 光学学报, 2021, 41(1): 0102002.

Research on Thermal-Frequency Characteristics of 633 nm Internal-Mirror He-Ne Laser

Xi Lu¹, Yin Cong^{1*}, Wang Jianbo¹, Shi Chunying¹, Cai Shan¹, Liu Ruonan^{1,2},
Li Mengyao^{1,3}, Zhang Chaochao^{1,2}

¹ Institute of Geometric Metrology Science, National Institute of Metrology, Beijing 100029, China;

² College of Metrology & Measurement Engineering, China Jiliang University, Hangzhou, Zhejiang 310018, China;

³ School of Optics and Photonics, Beijing Institute of Technology, Beijing 100081, China

Abstract

Objective In length measurement, the laser interferometer is used as the length-based standard at all levels, and the measured length value is calculated according to the emission wavelength of its light source. The stable and reliable output laser frequency (or wavelength) characteristics of various frequency stabilized lasers as the light source of the interferometer are the basic working conditions to ensure the normal operation of the interferometer. The 633 nm internal-mirror He-Ne laser with the double longitudinal mode power balance frequency stabilization principle is controlled based on the central frequency of the laser medium gain curve. However, the central frequency of the gain curve is affected by the air pressure in the tube. Therefore, the laser frequency after frequency stabilization is related to the gas pressure in the tube. For the full-cavity He-Ne laser tube, the change of the pressure in the cavity is mainly caused by the temperature change, and the pressure in the cavity increases linearly with the increase of temperature. Therefore, the frequency of the laser output is closely related to the temperature. As the frequency stabilized He-Ne laser is used more and more widely, there are higher requirements for the environmental adaptability of the frequency stabilized lasers. For example, the frequency stabilized He-Ne laser used in the laser interferometric absolute gravimeter needs to work at different ambient temperatures. Therefore, the frequency reproducibility of the current frequency stabilized He-Ne laser at extreme temperatures is greatly restricted.

Methods In this paper, the free-running characteristics of the 633 nm internal-mirror He-Ne laser tube at $-20\text{--}40\text{ }^{\circ}\text{C}$ are studied. According to these characteristics, a preheating and frequency stabilization control scheme of the laser system is designed, and the frequency stability of the 633 nm internal-mirror He-Ne laser is realized. When the room temperature is about $24\text{ }^{\circ}\text{C}$, the locked thermally stabilized laser beats with the high-precision iodine stabilized laser, and the relative standard uncertainty and Allen variance of the thermally stabilized laser are obtained. In addition, 6 sets of frequency reproducibility experiments are carried out in 3 months. The ambient temperature is $T = (24 \pm 2)\text{ }^{\circ}\text{C}$, and the measurement time is more than 1 h each time. The frequency reproducibility of the thermal frequency stabilization control system of the 633 nm internal-mirror He-Ne laser is investigated, and the influence of ambient temperature on the frequency stabilization results is studied. Different ambient temperatures for frequency stabilization experiments are set up. The ambient temperature is in $-20\text{--}40\text{ }^{\circ}\text{C}$ with an interval of about $20\text{ }^{\circ}\text{C}$. The temperature and beat values of the laser tube wall after frequency stabilization are measured at different ambient temperatures. At the same time, the pressure estimation model is used to estimate the frequency drift with ambient temperature after frequency stabilization, which is compared and verified with the experimental results.

Results and Discussions The free-running process of the laser tube at the ambient temperature of $-20\text{--}40\text{ }^{\circ}\text{C}$ is studied. The experimental results show that when the laser tube reaches the approximate thermal equilibrium state at different ambient temperatures, the voltage difference of the two longitudinal modes changes for 40 cycles (Fig. 5), and the thermal expansion rate of the cavity length is also the same, which shows that the ratio of heating to heat dissipation of the laser system is constant in the thermal equilibrium state. In addition, there is a linear relationship between the wall temperature of the laser tube and the initial ambient temperature after the system reaches the thermal equilibrium (Fig. 6), which shows that even if the laser is at different ambient temperatures, the heat exchange capacity between the laser system and the external environment is approximately unchanged, so the difference between the temperature of the wall of the laser tube and the initial ambient temperature is fixed when the system finally reaches the thermal equilibrium. In addition, the influence of ambient temperature on the frequency

stabilization results is investigated. The experimental results show that the temperature of the laser tube wall changes with the ambient temperature after frequency stabilization, and the relationship between them is linear (Fig. 11). At the same time, the drift of the laser output frequency with the ambient temperature after frequency stabilization is about 293 kHz/°C, which is consistent with the drift value of 268 kHz/°C calculated by the pressure estimation model. After linear interpolation calibration, the difference between the actual frequency value and the reference output frequency value is less than 1.81 MHz (Fig. 12).

Conclusions In this paper, the free-running characteristics of the 633 nm internal-mirror He-Ne laser tube at the ambient temperature of $-20\text{--}40\text{ }^{\circ}\text{C}$ are studied. The experimental results show that when the laser tube reaches the thermal equilibrium at different ambient temperatures, the difference between the laser tube temperature and the ambient temperature is fixed, the expansion rate is also the same, and the voltage difference of the double longitudinal mode changes for the same period. According to these characteristics, the preheating and frequency stabilization control scheme of the laser system is designed, and the frequency stabilization of the 633 nm internal-mirror He-Ne laser is realized. When the room temperature is about $24\text{ }^{\circ}\text{C}$, the beat frequency results of the locked thermally stabilized laser and the high-precision iodine stabilized laser show that the relative standard uncertainty of frequency within 3 h is $u = 6.4 \times 10^{-9}$. When the sampling time $\tau = 1\text{ s}$, the corresponding Allan variance is 7.0×10^{-11} . When $0.1\text{ s} \leq \tau \leq 2000\text{ s}$, the Allan variance is better than 4.3×10^{-10} , and the frequency reproducibility within 3 months is better than 4.6×10^{-9} . This paper also studies the frequency drift law of the output laser after locking at the ambient temperature of $-20\text{--}40\text{ }^{\circ}\text{C}$. The experimental results show that the temperature of the laser tube wall changes linearly with the ambient temperature after frequency stabilization. At the same time, the drift of the laser output frequency with the ambient temperature after frequency stabilization is about 293 kHz/°C, which is consistent with the drift value of 268 kHz/°C calculated by the pressure estimation model. In this regard, when the laser is working in a large temperature range (such as $-20\text{--}40\text{ }^{\circ}\text{C}$), interpolation calibration can be used to obtain a more accurate reference output frequency.

Key words lasers; internal-mirror He-Ne laser; double longitudinal mode; power balance; high and low temperature test; frequency drift